J Electroceram (2006) 16:489–493
DOI 10.1007/s10832-006-9903-3

Study of nanocrystal TiO_2 thin films by thermal annealing

Z. W. Zhao · B. K. Tay

Abstract The amorphous films were annealed in a wide temperature range (250–1000°C) and film properties of TiO_2 thin films were studied. Nano-sized anatase polycrystallites had been induced by thermal annealing for the films annealed at and above 300°C as confirmed by X-ray diffraction. Strong LO-phonon Raman modes, especially B_{1g} (395 cm^{-1}) and E_g (636 cm^{-1}) in Raman spectra and the absorption peak at 436 cm^{-1} in absorbance spectra by Fourier transform infrared spectroscopy also indicated the existence of anatase phase in crystalline thin films. In addition, with the increase of the annealing temperature, the wettability of the film surface was enhanced as shown by the decrease of water contact angle from over 90° to less than 40°. Moreover, upon UV laser irradiation on film surface, the water contact angle saturated at 10° indicative of a highly hydrophilic surface for all the films, which arose from the dissociative adsorption of water molecules on the defect sits of the surface generated by the photocatalysis reactions of TiO_2. This behavior makes the film a good potential candidate for self-clean coatings.

Keywords Anatase · Raman scattering · FTIR · photocatalysis

1 Introduction

Nanocrystal ceramics with average grain sizes of less than 100 nm are beginning to get considerable research interest due to the improvement in a variety of properties that are expected to result from grain-size refinement to the nanometer scale [1]. It is used potentially in a variety of catalytic, electronic, and magnetic applications, as well as precursors in net-shape formed ceramic components. Nanocrystal titanium dioxide (TiO_2), as one of the most popularly ceramic materials, has been widely used because of its high refractive index, high dielectric constant, high chemical stability, and excellent transparency in the visible and near-infrared bands [2].

A wide variety of techniques and methods are reported to prepare nanocrystal TiO_2. For example, the study on the crystal TiO_2 films could be found in the literature [3–5] by using metal organic chemical vapour deposition (MOCVD) and magnetron sputtering. Besides, TiO_2 with nano-powders could be synthesized by gas condensation [1]. Furnace annealing, as a convenient and low-cost method, has also been widely used to obtain crystalline materials [6–8]. However, using this method seldom work was reported on the properties of nanocrystalline TiO_2 thin films by filtered cathode vacuum arc (FCVA), which is a promising technique to deposit dense thin films with high quality [9, 10]. Thus, in this work, post-annealing of TiO_2 thin films by FCVA was carried out. It was found that nanocrystal TiO_2 could be easily obtained in a wide temperature range with pure anatase phase. Compared with rutile TiO_2, antase TiO_2 is preferred for the applications based on the combination of (electro)chemical reactions at the surface and transport of electrons and ions through the bulk of the material. In this article, film properties including structure evolution and photocatalysis effect by UV irradiation will be investigated in detail.

2 Experimental details

Titanium dioxide thin films were deposited by as described in detail elsewhere [9]. The films were grown on Si (100) substrates at room temperature with the growth pressure of 3×10^{-4} Torr. The as-grown films were then cut into several

Z. W. Zhao (✉) · B. K. Tay
School of Electrical and Electronic Engineering, Nanyang Technological University, Singapore 639798
e-mail: ezwzhao@ntu.edu.sg

parts and annealed at 250, 300, 500, 800 and 1000°C for 1 h in a quartz furnace in air, respectively. The crystalline structures of the films were measured by X-ray diffraction (XRD). The Raman spectra were excited using 514.5-nm line of an Ar^+ laser and collected in a backscattering geometry on a CCD camera using a Renishaw micro-Raman System 1000 spectrometer. Laser power on the sample was less than 2 mW. Fourier transform infrared spectroscopy (FTIR) spectra were obtained at room temperature in the range of 350 to 1000 cm^{-1}. The surface morphology was measured by atomic force microscopy (AFM) in tapping mode (Dimension 3000).

Film surface wettability was evaluated by measuring the contact angle for water droplets before and after UV irradiation. UV irradiation was carried out by the 244 nm line from a frequency-doubled argon laser with different irradiation times with the power density lower than 1 w/cm^2 on film surface. The contact angle measurements of the thin films were carried out in atmospheric conditions at 25°C using VCA Optima device from AST Products, Inc. For each sample, at least three drops were measured. The accuracy of the contact angle is less than 1°.

3 Results and discussion

3.1 XRD analysis

Figure 1 shows the XRD results of TiO_2 films after annealed at different temperatures by thermal annealing. The as-grown film was amorphous and the structure remained up to 250°C as no peak could be found in XRD patterns as shown in curves (a) and (b). A peak at $2\theta = 25.4°$ with a strong reflection from (101) plane was observed in the XRD patterns for the films annealed at and above 300°C, which implied the onset temperature of crystallization occurred at 300°C. Besides, several other peaks including (200), (105) and (211) orientation planes from anatase phase in curves (c)–(f) were also observed, indicating the existence of polycrystallites in these films. It was also found that the intensity of the peaks generally increased as increasing the annealing temperature, suggesting the enhancement of crystallinity of the films. No rutile TiO_2 was observed for these crystalline films. The average crystallinity size of the films was evaluated to be less than 30 nm by using Scherrer's equation [11] and no significant changes were noticed in crystallinity size for the films annealed at various temperatures.

3.2 Raman scattering analysis

Raman spectra for the as-grown and annealed films were shown in Fig. 2. The frequency and assignment of the Raman bands of anatase and rutile titania could be found in the literature [9]. No Raman peaks could be observed for the as-grown film and the film annealed at 250°C. Above 250°C, several separate peaks with differently relative intensity were observed as shown in curves (b)–(d). From the Raman spectra, it indicated that the transition from amorphous state to crystalline occurred at 300°C, being as same as that in previous XRD analysis. The appearance of film crystallization was believed to be induced by thermal annealing. All the spectra of annealed films above 250°C showed similar features. The intense 520 cm^{-1} peak and the weak broad one at 300 cm^{-1} were originated from silicon substrate as well as the peak around 950 cm^{-1}. Other peaks were ascribed to the Raman-active vibrational modes from anatase in crystalline films. All the Raman allowed vibrational modes for anatase titania were observed for crystalline films, except for the E_g mode at 515 cm^{-1} suppressed by the strong LO-phonon line of silicon at 520 cm^{-1}. The strong intense peaks around 394 and

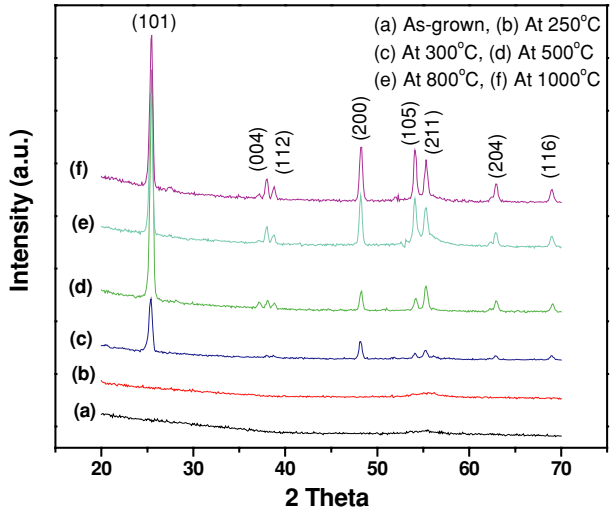

Fig. 1 XRD patterns for the as-grown and annealed TiO_2 thin films

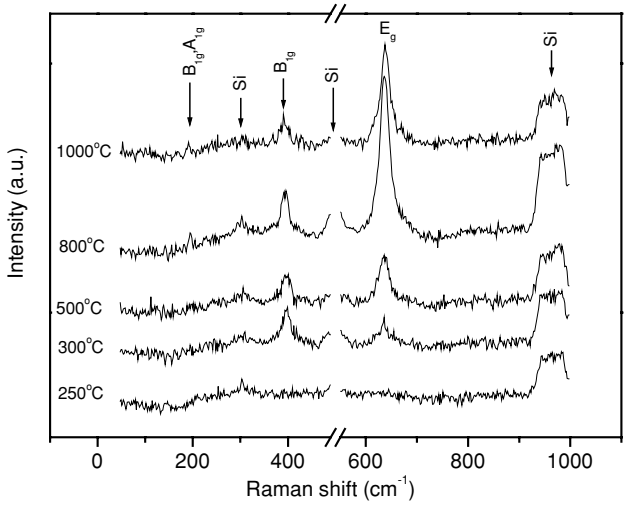

Fig. 2 Raman scattering spectra for the as-grown and annealed TiO_2 thin films

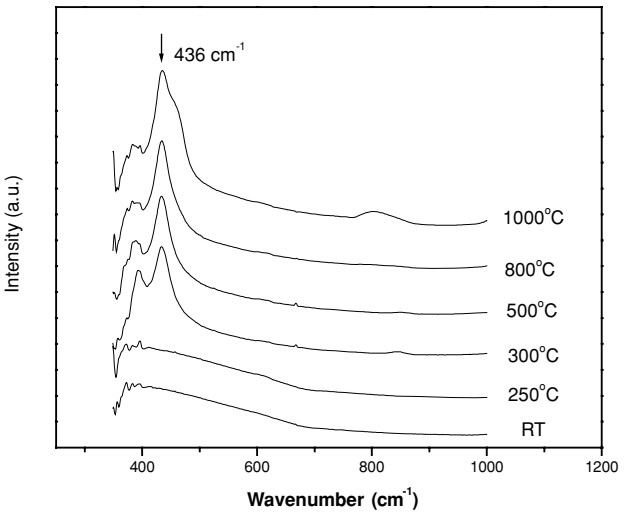

Fig. 3 FTIR spectra for TiO_2 thin films

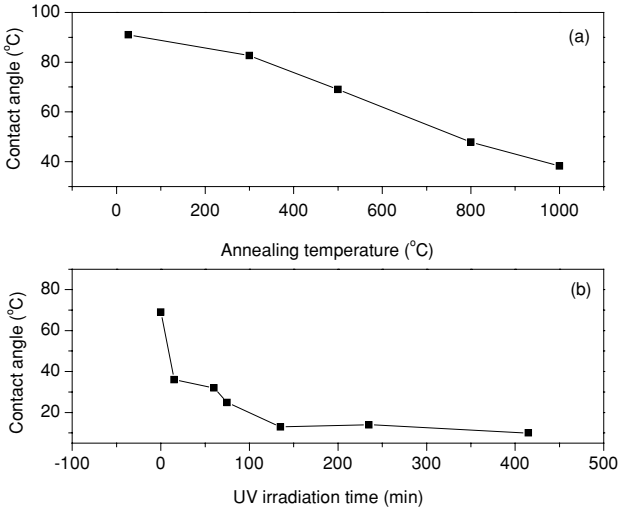

Fig. 4 (a) Variation of contact angle for various thin films with annealing temperature; (b) Dependence of contact angle for the film annealed at 500°C on irradiation time under the laser line of 244 nm

636 cm^{-1} were assigned to anatase B_{1g} and E_g LO-phonon modes, respectively. Another weak peak at 197 cm^{-1} was originated from anatase (B_{1g}, A_{1g}) LO-phonon modes.

3.3 FTIR analysis

Figure 3 shows the absorbance spectra of annealed films together with the as-grown one measured by FTIR. Obviously, below 300°C, no observed absorption peak from the film implied amorphous films. Above 250°C the annealed films exhibited the similar peaks around 436 cm^{-1}, which was the typical characteristic of Ti-O-Ti transverse mode of anatase [12]. Another peak around 388 cm^{-1} could also be detected below the peak of 436 cm^{-1}. However, the origin of it remained unknown as it ascribed to neither anatase nor rutile TiO_2. The occurrence of anatase phase above 250°C was agreed well with previous analysis from the XRD patterns (Fig. 1) and Raman spectra (Fig. 2).

3.4 Photocatalysis analysis

The water contact angles for the films annealed at different temperatures were measured and shown in Fig. 4(a) as a function of annealing temperature. Usually, a hydrophilic surface has a contact angle less than 70°, and a hydrophobic surface is characterized by a contact angle of 70° or above [13]. The contact angle for the as-grown film was around 90°, higher than those of annealed films, suggesting the characteristic of preferred hydrophobic surface. For the film annealed at 300°C, the contact angle decreased to 80° and further decreased to less than 40° at 1000°C. The reduction of contact angle as increasing the annealing temperature suggested that the film surface turn from hydrophobicity to hydrophilicity. It is well known that the contact angle is closely related to the surface morphology. The correlation between surface roughness and contact angle could be described by the equation as below [14]:

$$r(\gamma_{sv} - \gamma_{sl}) = \gamma_{lv}\cos\theta_w \quad (1)$$

Where, r is the roughness factor defined as the ratio of the real and the apparent surface areas; γ_{sv} is the solid surface energy; γ_{sl} is the solid-liquid surface energy and θ_w is the contact angle for the wetting of a rough surface. Clearly, as shown by the equation, the rougher the contact surface, the smaller the contact angle will be. Thus, surface morphology of the films was conducted by AFM as shown in Fig. 5. Obviously, the surface morphology of the films remarkably differed from each other. The surface roughness for the as-grown film was very smooth (less than 0.1 nm in terms of root mean square in figure a). When the annealing temperature increased, the film surface became rougher and the value of root mean square remarkably increased up to 9 nm at 1000°C, concurrent with the sharp increases of the vertical scale bar as shown in Figs. 5(b) and (c). Evidently, the significant increase in surface roughness could contribute to the decrease of contact angle with the increase of annealing temperature.

Upon the UV light irradiating the sample surface, the water contact angle for all the samples monotonously decreased with the increase of irradiation time. This behavior was especially significant at the early stage of the irradiation time of 15 min with sharply decreased contact angle. After irradiation time of 60 min, all the films were hydrophilic. For example, as shown in Fig. 4(b), the contact angle of the film annealed at 500°C decreased to 36° within the UV irradiation of 15 min, indicating the surface had converted from hydrophobicity to hydrophilicity in such a short irradiation time. Further increasing the irradiation time, contact angle decreased

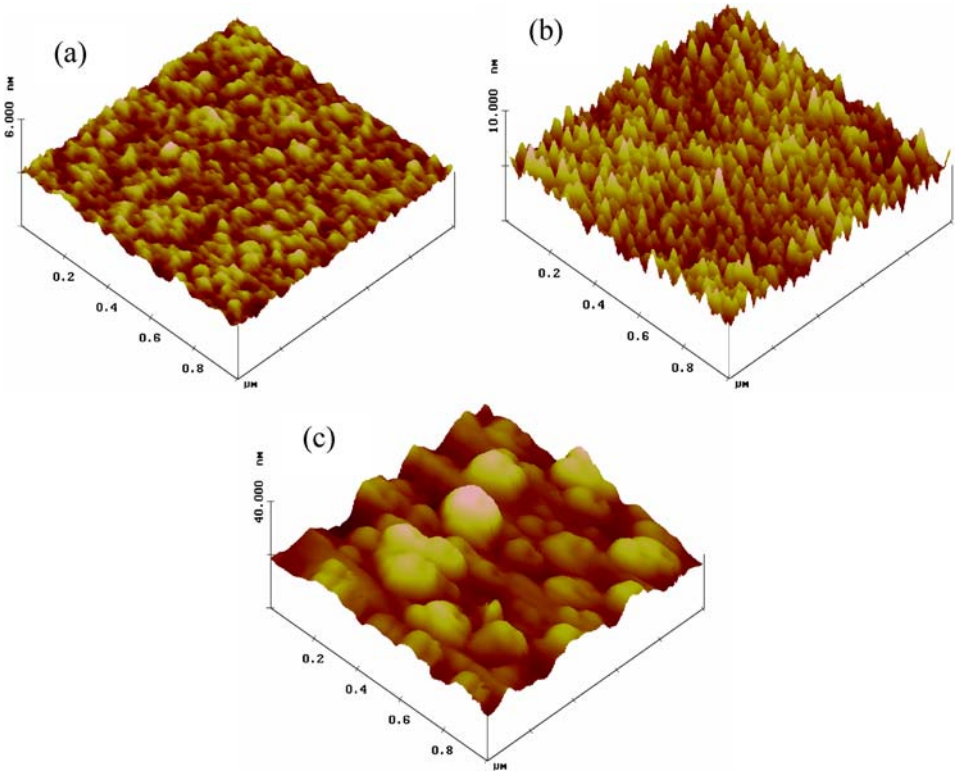

Fig. 5 AFM images for (a) as-grown film, and the films annealed at (b) 500°C and (c) 800°C

slowly and eventually saturated at 10°, implying the highly hydrophilic surface of the film. No obvious difference in contact angle among the various samples was observed after a prolonged time of UV irradiation. Yu et al. [15] also observed the similar trend, where the contact angle changed from around 50° at initial state to around 10° after irradiation.

It is well known that TiO_2 has a band gap of ~3.2 eV and electron-hole pairs would generate under such a band gap illumination. These photo-generated electrons (e^-) and holes (h^+) could either recombine or move to the surface to react with the species adsorbed on the surface known as the basis of photocatalysis [16, 17]. The holes would react with the oxygen from TiO_2 lattice, giving rise to the formation of surface oxygen vacancies. Meanwhile, some of the electrons react with lattice Ti^{4+}, leading to Ti^{3+} defect sites. Such a process including the generation of the defect sites (e.g. the conversion of Ti^{4+} sites to Ti^{3+} sites and the creation of oxygen vacancies) on the film surface could be expressed as below [18, 19]:

$$TiO_2 + 2\,h\nu \rightarrow 2\,h^+ + 2e^- \quad (2)$$

$$O^{2-} + 2\,h^+ \rightarrow 1/2O_2 + \square\ \text{(oxygen vacancy)} \quad (3)$$

$$Ti^{4+} + e^- \rightarrow Ti^{3+}\text{(surface trapped electron)} \quad (4)$$

Upon UV irradiation, the surface trapped electrons (Ti^{3+}) would react with oxygen molecules adsorbed on the film surface, forming lattice ions (Ti^{4+}) and O_2^-. Meanwhile, water molecules were dissociatively adsorbed on the film surface to form single coordinated or doubly coordinate surface hydroxyls into the oxygen vacancies. During these processes, the competition between water and oxygen to dissociatively adsorb on the defect sites would occur. UV illumination in air would enhance water adsorption than oxygen adsorption. In other words, hydroxyl absorption is more favorable than that of oxygen [20]. Consequently, water molecules could favorably occupy oxygen vacancies, resulting the decrease of water contact angle and therefore the highly hydrophilic surface.

4 Conclusions

The properties of TiO_2 thin films were investigated under various annealing temperatures. It was found that crystallization was induced by thermal annealing above 250°C and confirmed by XRD, Raman scattering and FTIR spectra, where only anatase phase was observed for the films annealed at and beyond 300°C. Photocatalysis of amorphous and crystallized TiO_2 films were also investigated under UV laser irradiation. Before irradiation, the water contact angle of the films decreases as increasing the annealing temperature, tending to give a hydrophilic surface. At the early stage of irradiation time, contact angles for the all samples sharply decreased and saturated at 10° beyond 400 min to show the highly hydrophilic surface. No obvious deviation of the contact angles

for all the samples could be observed after prolonged irradiation time.

References

1. J.A. Eastman, *J. Appl. Phys.*, **75**, 770 (1994).
2. J.D. DeLoach and C.R. Aita, *J. Vac. Sci. Technol.*, **A16**, 1963 (1998).
3. K. Okimura, *Surf. Coat. Technol.*, **135**, 286 (2001).
4. T.M.R. Viseu, B. Almeida, M. Stchakovsky, B. Drevillon, M.I.C. Ferreira, and J.B. Sousa, *Thin Solid Films*, **401**, 216 (2001).
5. M.K. Lee, Y.M. Hung, and J.J. Huang, *Jpn. J. Appl. Phys.*, **40**, 6543 (2001).
6. Y.M. Kang, S.H. Wee, S.I. Baik, S.G. Min, S.C. Yu, S.H. Moon, Y.W. Kim, and S.I. Yoo, *J. Appl. Phys*., **97**, 10A319 (2005).
7. R. Puthenkovilakam, Y.S. Lin, J. Choi, J. Lu, H.O. Blom, P. Pianetta, D. Devine, M. Sendler, and J. P. Chang, *J. Appl. Phys.*, **97**, 023704 (2005).
8. S.Y. Shao, J.D. Shao, D.P. Zhang, J.B. Huang, and Z.X. Fan, *Proc. SPIE Int. Soc. Opt. Eng*., **5774**, 307 (2004).
9. Z.W. Zhao, B.K. Tay, and G.Q. Yu, *Appl. Optics*, **43**, 1281 (2004).
10. Z.W. Zhao, B.K. Tay, G.Q. Yu, and S.P. Lau, *J. Phys.: Conden. Mat.*, **15**, 7707 (2003).
11. B.D. Cullity, *Elements of X-ray Diffraction*, 2nd edn. (Addison Wesley, Reading. MA, 1978), p. 102.
12. C. pecharromán, F. Gracía, Juan P. Holgado, M. Ocanaña, Agustín R. González-Elipe, J. Bassas, J. Santiso, and A. Figueras, *J. Appl. Phys*., **93**, 4634 (2003).
13. S. Adachi, T. Arai, and K. Lobayashi, *J. Appl. Phys.*, **80**, 5422 (1996).
14. A.W. Neumann, *Adv. Coll. Interf. Sci.*, **4**, 438 (1974).
15. J.C. Yu, W. Ho, J. Lin, H. Yip, and P.K. Wong, *Envir. Sci. Technol.*, **37**, 2296 (2003).
16. A. Fujishima, K. Hahimoto, and T. Watanabe, *TiO_2 Photocatalysis: Fundamentals and Applications* (BKC. Inc., Tokyo, Japan, 1999).
17. N. Serpon and E. Pelizzetti, *Photocatalysis Fundamentals and Applications* (Wiley-Interscience, Amsterdam, 1989).
18. R.D. Sun, A. Nakajima, A. Fujishima, T. Watanabe, and K. Hashimoto, *J. Phys. Chem.*, **B105**, 1984 (2001).
19. M. Miyauchi, A. Nakajima, A. Fujishima, K. Hashimoto, and T. Watanabe, *Chem. Mater.*, **12**, 3 (2000).
20. R. Wang, N. Sakai, A. Fujishima, T. Watanabe, and K. Hashimoto, *J. Phys. Chem*., **B103**, 2188 (1999).